TILT ROTOR AERODYNAMICS: A COMPARATIVE STUDY OF A BEM METHODOLOGY WITH THE PROPWING DATABASE

A. Visingardi
CIRA - Centro Italiano Ricerche Aerospaziali
Capua (CE) - Italy

Abstract

The present paper illustrates an aerodynamic analysis performed by CIRA in the framework of the European research project TILTAERO (TILTrotor interactional AERODynamics) by the application of a BEM methodology and with the aim to investigate the problem of the interactional aerodynamics of a tilt rotor configuration. Due to the lack of experimental database on tilt rotor configurations the one produced during the European research project PROPWING and referring to a propeller-nacelle-wing configuration has been chosen for the numerical-experimental comparison activity. The paper provides a synthetic description of the TILTAERO project and illustrates the main aspects of the PROPWING configuration and the relative experimental database. The main features of the numerical methodology applied is also described. The comparative study is performed by illustrating the numerical and experimental results in terms of steady, time-averaged and unsteady pressure distribution as well as steady and time-averaged normal forces acting on the wing. The results obtained indicate, in general, a satisfactory agreement of the methodology applied with the experiment.

List of symbols

c	Chord of the wing, m
CN	Wing sectional normal force coefficient $(=(dN/dy)/q_\infty c)$
Cp	Wing sectional pressure coefficient $(=(p-p_\infty)/q_\infty)$
CQ	Propeller torque coefficient $\left(=Q/\left(\pi\rho_\infty\Omega^2R^5\right)\right)$
CT	Propeller thrust coefficient $(=T/(\pi\rho_\infty\Omega^2R^4))$
D	Propeller diameter, m
N	Wing sectional normal force, N
p	Local static pressure, N/m^2
p_∞	Free-stream static pressure, N/m^2
q_∞	Free-stream dynamic pressure $(=1/2\,\rho_\infty V_\infty^2)$, N/m^2
Q	Propeller torque, Nm
R	Propeller radius, m
T	Propeller thrust, N
V_∞	Free-stream velocity, m/s
x	Wing chordwise coordinate, m
y	Wing spanwise coordinate, m
θ_N	Nacelle tilt angle, degrees
ρ_∞	Free-stream density, kg/m^3
ψ	Propeller azimuthal angle, degrees
Ω	Propeller angular velocity, RPM
$\_AVE$	Indicates time-averaged components
$\_IND$	Indicates induced components
$\_u$	Indicates unsteady components

Introduction

The tilt rotor is an aircraft which combines the advantages of vertical takeoff and landing capabilities, specific to the helicopters, with the forward speed and range of a turboprop airplane. Such characteristics make this aircraft able to provide high-speed, long-range flight, coupled with runway independent operations thus having a significant potential to considerably reduce airport congestion problems. These attractive peculiarities have constituted the guideline of the US research for more than forty years during which a huge experience has been matured both in the experimental and in the theoretical fields. Unlike the US, the European interest in this configuration is only very recent and for this reason the European helicopter community suffers from a lack of both experimental and

theoretical experience. In order to increase the competitiveness of the European helicopter industry a series of European Union-funded research projects has been launched which investigate the various technological aspects dealing with the tilt rotor aircraft.

The TILTAERO project

In this framework, the four-year research project TILTAERO (TILTrotor interactional AEROdynamics), funded by the European Union under the "Competitive and Sustainable Growth" Programme, Contract Nr. G4RD-CT-2001-00477, [Ref.1], aims at the development of a common European database capable to cover the main aerodynamic interactional phenomena arising during the different flight conditions of a tilt rotor aircraft. This database is employed to validate the prediction tools in order to assess their capabilities in capturing the interactional phenomena and to address the research activity to those areas revealing lack of knowledge.

The research objectives addressed by the TILTAERO project will provide:

- a range of high performance and validated analytical tools that will enable designers to accurately predict the aerodynamics efficiency of the tilt rotor wing surfaces (fixed and rotating);

- a detailed investigation of the aerodynamic interactional phenomena in different tilt rotor flight conditions, providing high quality wind tunnel test data to increase the designer's knowledge about aircraft efficiency in this field.

The consortium includes the four European helicopter manufacturers: Agusta S.p.A. (Italy), co-ordinator of the project; Westland Helicopters Ltd (UK); Eurocopter (France) and Eurocopter Deutschland (Germany); the IAI, Israel's aircraft manufacturer; four aerospace research centres: CIRA (Italy); DLR (Germany); NLR (The Netherlands) and ONERA (France), and the National Technical University of Athens, NTUA (Greece).

The project is organised in five work packages: WP1 - Aerodynamics Prediction Codes; WP2 - Powered full-span mock-up feasibility studies; WP3 - Powered half-span mock-up; WP4 - Wind Tunnel tests of the powered half-span mock-up; WP5 - Wind Tunnel tests analysis.

A large variety of prediction tools is available among the participating partners: from Flight Mechanics codes to panel methods, to the more sophisticated CFD Euler and Navier-Stokes computer codes. These existing tools, basically conceived for the aerodynamic analysis of the helicopters, have been critically assessed. A pre-test activity, aimed at assessing the ability of some of these tools, has been started by exploiting a database pre-existing to the present project. In particular, the database produced during the EU-funded research project PROPWING, [Ref.2], has been chosen for comparison purposes with the numerical results produced by the TILTAERO partners participating in this pre-test phase.

The aim of this paper is to illustrate the results so far obtained in the pre-test activity by CIRA. For this purpose, the PROPWING configuration and the relative experimental database is first described. The numerical methodology applied by the author is then illustrated and finally the results of the comparisons are illustrated and discussed.

The PROPWING database

Due to the lack of experimental database on tilt rotor configurations a search for an equivalent database has been conducted in TILTAERO which could refer to a configuration having close phenomenological similarities with a tilt rotor aircraft. The database produced during the research project PROPWING [Refs.3,4,5] has been recognized as the most appropriate to be employed.

The PROPWING wind tunnel tests aimed at providing a database of aerodynamic measurements relative to a propeller-wing interactional condition for two different configurations: one corresponding to a conventional case of a propeller aircraft (PNW configuration) and one corresponding to a tilt-rotor aircraft (PNW/2 configuration). Both

configurations were tested in the S1-Luminy wind tunnel in Marseilles. In particular, referring to the PNW/2 configuration, the one analysed during the TILTAERO pre-test activity, a closed test section of octagonal shape of total area 7.45m^2 was employed.

The PNW/2 model

The model (Fig.1) was equipped with a 4-bladed Marquis propeller scaled down to a diameter D=0.85m. The propeller sense of rotation was such that the inboard blade was moving upward. Airfoils of the NACA64AXX series composed the blades. The wing had a rectangular planform formed by the RA18-43N$_1$L$_1$ airfoil section, which is used on the ATR42 of Aerospatiale. The chord was c=1.02m (1.2D) and the span was equal to 0.75m (Fig.2).

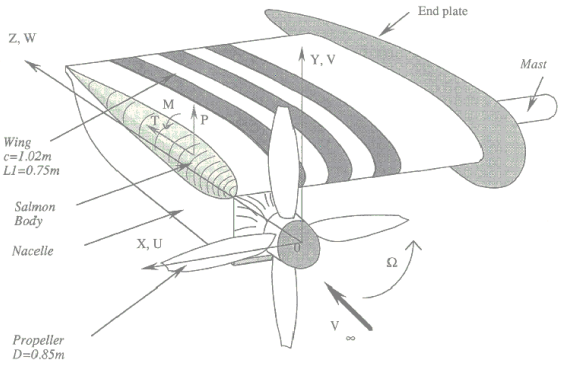

Figure 1: The PNW/2 configuration

The propeller was placed at the tip of the wing. The nacelle covered a width of 0.2m and was scaled down from the real nacelle of the ATR42. A fairing (salmon) was placed at the tip. The propeller was able to tilt, together with the nacelle, with respect to the wing. Four tilt angles were considered: θ_N=0^0, 30^0, 60^0 and 90^0 .

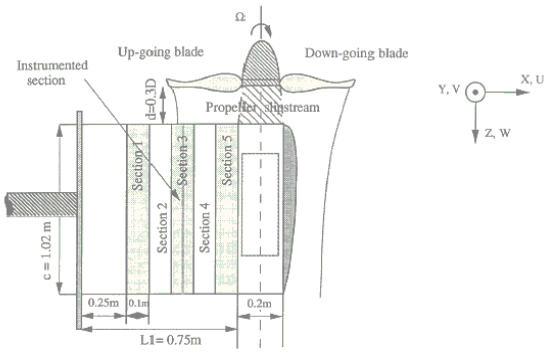

Figure 2: Basic dimensions of the PNW/2 configuration

The measurement techniques

The global forces were measured using strain gauges on the support of the configuration. By disengaging the wing from the support, the global forces corresponded to the rest of the configuration; Thus, the induced effect on the propeller was also estimated. Mean and instantaneous pressure distributions on the wing were measured using pressure taps placed at 5 instrumented sections located, with respect to the propeller axis of rotation, at 0.15m (section 5), 0.25m (section 4), 0.35m (section 3), 0.45m (section 2) and 0.55m (section 1). Twenty pressure taps were located on each instrumented section. Velocity measurements were carried out by means of hot-wire anemometry. A x-probe was used: by rotating it all the three velocity components were then measured. The hot-wire anemometry was also used in order to determine the tip vortex evolution.

The experimental database

Averaged and unsteady measurements are available on this configuration both in propeller-off mode (NW/2) and propeller-on mode (PNW/2) in terms of global forces, sectional forces and pressure distributions. The tip vortex paths were measured downstream of the propeller for 0^0 and 30^0 nacelle tilt. Furthermore, the mean and instantaneous velocity fields were also measured at a mid-chord cross section.

Description of the methodology applied

The in-house developed CIRA computer code RAMSYS (Rotorcraft Aerodynamic Modelling SYStem), [Ref.6], is an unsteady panel code for multi-body configurations based on Morino's boundary integral formulation. The formulation consists in the solution of Laplace's equation written in terms of the velocity potential φ :

$$\nabla^2\varphi = 0 \qquad \forall x \notin S(t) \qquad (1)$$

such that $\mathbf{v} = \nabla\varphi$. $S(t)$ is a surface outside of which the flow is potential and consists of a surface S_B surrounding the body geometry and a surface S_W surrounding the wake geometry.

The boundary condition at infinity is that $\varphi = 0$. The surface of the body is assumed to be impermeable hence $\frac{\partial \varphi}{\partial n} = \mathbf{V}_B \cdot \mathbf{n}$ where $\mathbf{V}_B$ is the velocity of a point on the body. The wake is a surface of discontinuity which is not penetrated by the fluid and across which there is no pressure jump. The second wake condition implies that $\Delta\varphi$ remains constant following a wake point x_W, and equal to the value it had when x_W left the trailing edge. The value of $\Delta\varphi$ at the trailing edge is obtained by using the Kutta-Joukowski hypothesis that no vortex filament exists at the trailing edge; this implies that the value of $\Delta\varphi$ on the wake and the value of $\Delta\varphi$ on the body are equal at the trailing edge.

The application of Green's function method to Eq.(1), yields the following boundary-integral-representation for the velocity potential φ:

$$E(x_*)\varphi(x_*,t_*) = I_B + I_W \qquad (2)$$

with

$$I_B = \iint_{S_B}\left[\left(-\frac{1}{4\pi\rho}\right)\frac{\partial\varphi}{\partial n} - \varphi\frac{\partial}{\partial n}\left(-\frac{1}{4\pi\rho}\right)\right]dS$$

and

$$I_W = -\iint_{S_W}\Delta\varphi\frac{\partial}{\partial n}\left(-\frac{1}{4\pi\rho}\right)dS$$

representing respectively the contribution of the body and the wake. E_* is a domain function defined as zero inside S and unity elsewhere.

The helicopter geometry and the wake are respectively discretised by M and N hyperboloidal quadrilateral panels, on which the unknown velocity potential, the normal-wash and the velocity potential jump are constant (zeroth-order formulation).

Using the collocation method and setting the collocation points at the centroids of each element on the body geometry, the integral equation, Eq.(2), is replaced by an algebraic linear system of equations for the velocity potential φ:

$$E_k\varphi_k(t) = \sum_{m=1}^{M} B_{km}\psi_m(t) + \sum_{m=1}^{M} C_{km}\varphi_m(t) + \sum_{n=1}^{N} F_{kn}\Delta\varphi_n(t) \qquad (3)$$

where B, C, and F are respectively the body source, body doublet, and wake doublet influence coefficients. A Conjugate Gradient Method (GMRES solver) is applied for the numerical solution of the problem.

A correction of the *classical* Kutta condition [Ref.7] is implemented in the code in order to guarantee a zero pressure jump at the trailing edge.

A time-marching free-wake model is implemented in RAMSYS. Wake panels are released at each time step from the trailing edge as the lifting body moves through an inertial frame of reference. Therefore, the shape of the wake is a consequence of the local induced velocities which are evaluated from Eq.(2) as:

$$\mathbf{v}_i = \iint_{S_B}\left[\left(-\frac{\boldsymbol{\rho}}{4\pi\rho^3}\right)\frac{\partial\varphi}{\partial n} - \varphi\frac{\partial}{\partial n}\left(-\frac{\boldsymbol{\rho}}{4\pi\rho^3}\right)\right]dS - \iint_{S_W}\Delta\varphi\frac{\partial}{\partial n}\left(-\frac{\boldsymbol{\rho}}{4\pi\rho^3}\right)dS \qquad (4)$$

Different vortex-core models are available to stabilize the wake.

Interactional Technique: The simple use of free-wake modelling can be successfully employed for flight conditions where the interactions between the wake and the rotor are relatively mild. However, for strong interactions in which the wake penetrates the body surface this approach leads to unphysical solutions. The present version of RAMSYS implements the method proposed by Clark and Maskew [Ref.8] for body/wake

interactions. The method poses its fundamentals on an interpretation of flow visualization data relative to a tip vortex filament approaching and then intersecting a body. As the vortex approaches the body it starts to deform about the body shape and the deformation continues until when the vortex elements which reach the closest proximity to the body disappear in the visualization. What happens to these elements is not very clear, nevertheless the remaining part of the vortex seems to continue to move downward but with a minor local distortion.

The numerical translation of this experience has consisted in simply cancelling the doublet intensities $\Delta\varphi$ of those wake panels which penetrate the body but allowing that the same wake panels could regain their intensity if during their motion downward they move outside of the body. The described procedure determines in the wake holes delimited by raw-edges corresponding to vortex segments. If these segments are too close to the body they can induce excessive velocities in the near body panels. For this reason a *safety distance* from the body is then computed with which all the wake panels lying inside it are also cancelled.

Wake Smoothing: The numerical analysis of rotor/body interactions by panel methods requires an opportune coupling between an interactional technique and a proper free-wake modelling. Indeed, if the interactional technique is necessary to avoid non physical overshoots in the solution, a correct free-wake displacement is crucial in evaluating the correct pressure distributions acting on the body.

The application of the pure free-wake model can determine an excessively chaotic vortical system which alters considerably the solution on the body. In order to regularize the wake shape a simple progressive stiffening technique and a smoothing technique have been applied. The progressive stiffening technique consists in evaluating the induced velocities acting on the wake panel nodes as a weighted average between the free-wake induced velocity field and the induced velocity field computed by applying the momentum theory to an isolated rotor. Two cubic polynomials function of the vortex age are used as weighting functions. The smoothing technique is employed in order to avoid the excessive deformation of the wake panels. The technique applied is based on the concept of the elastic membrane. For each wake node i a set of additional velocities are computed according to the expression:

$$\mathbf{V}_{e_{ij}} = \frac{K}{\Delta t}\mathbf{X}_{ij} \qquad (5)$$

being K a user-defined coefficient and $\mathbf{X}_{ij}$ the distance between the i-node and each of the four surrounding j-nodes. The computed velocities $\mathbf{V}_e$ are such that the net value $\sum_i \sum_j \mathbf{V}_{e_{ij}} = 0$

Results and Discussion

Model set-up

The flight condition chosen for the present numerical/experimental comparisons refers to the PNW/2 configuration set at zero angle of attach with a nacelle tilt angle equal to 30^0. The propeller angular velocity is equal to 1362 RPM and the free stream velocity is 17,20 m/s. The blade pitch is set at $32{,}5^0$.

Numerical discretization

The computations have been performed with a body (wing+nacelle) discretization equal to 2694 panels whereas each blade has been discretized by 32x12 panels. The azimuthal discretization has been fixed at 5^0.

Analysis of the results

A first set of numerical/experimental comparisons has been made with reference to the propeller-off configuration (NW/2) in order to evaluate the role played by the presence of a nacelle set at a high angle of attack and located in the close proximity of the wing tip. In particular, the analysis performed has highlighted the important role played by the wake shed from the nacelle. Results obtained neglecting the wake trailed from the side of the nacelle in contact with the wing tip have indicated the origin of an unnatural

expansion on the lower part of the wing in the proximity of the nacelle (Fig.3).

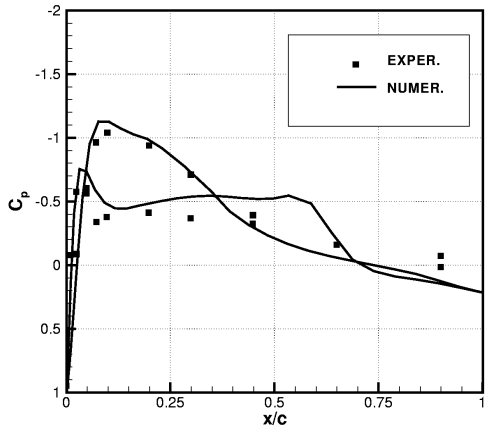

Figure 3: Unnatural expansion resulting from an incorrect nacelle wake modelling.

This expansion has been explained by the presence of an outflow at the wing tip which, in reality, is counteracted by the presence of a nacelle wake system. In order to overcome this problem the vortex shedding from the nacelle surface has been taken into account in the numerical simulations. Figure 4 illustrates a comparison in terms of the wing spanwise velocity at section 5 between the old nacelle wake modelling and the new one. The counteraction introduced by the new wake modelling is confirmed, in particular, by the inversion of direction of the velocity on the lower side of the wing section.

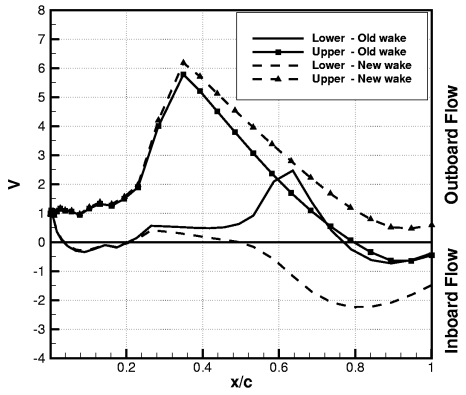

Figure 4: Outflow at wing tip

The results obtained by the application of this wake modelling are shown in Fig. 7 and indicate a generally satisfactory solution to the problem. However, the slight numerical over-prediction of ΔCp in the second half of the chordwise pressure distribution indicates the need of a further investigation of the problem.

The pressure distributions on the wing of the propeller-on configuration have been then evaluated. In order to better analyse the numerical results the time-averaged pressure distributions and the unsteady pressure distribution time histories have been separately represented.

The computed time-averaged pressure distributions show qualitative similarities to those obtained for the propeller-off configuration. In addition, a slight under-prediction of the suction peak at section 4 is also visible.

A comparison with results obtained by Agusta employing the VSAERO© [Ref.9] commercial code has been also made. The wing+nacelle geometry is discretized by 5362 panels and the rotor is modelled as an actuator disc discretized by 192 panels. The rotor wake employed is a closed-tube wake model usually applied in VSAERO© for bluff body geometries. The comparison between the numerical and experimental results (Fig.8) indicate a fair agreement up to section 4. Discrepancies between the Agusta results and the experiment are visible in section 5 where the use of a non-appropriate wake modelling (which is generated just by the wing and nacelle trailing edges) determines the same problems discussed for the propeller-off configuration.

An analysis in terms of the time-averaged sectional normal forces acting on the wing sections has been performed for both the propeller-off (NW/2) and propeller-on (PNW/2) configurations. Figure 5 illustrates the comparison between the numerical and experimental results.

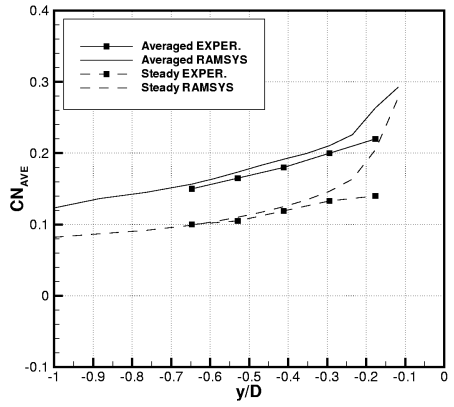

Figure 5: Normal force coefficient distribution on the wing

The presence of the nacelle at high angle of attack determines a progressive increase in the load from the wing root to the wing tip. The presence of the propeller with its sense of rotation determines an increase in the local effective angles of attack of the wing sections and thus increasing the normal forces. The numerical investigation indicates both a qualitative and quantitative agreement with the experiment up to section 4. An excessive over-prediction at section 5, the one close to the nacelle, can instead be noticed.

The unsteady component of the pressure distributions have been then evaluated. A selection of eight significant pressure tap locations (out of the twenty available per wing section) has been made in order to draw general guidelines of the unsteady propeller wake-wing interactional phenomenology. The choice has been made by considering three main regions of the wing section: a) the leading edge; b) the central region; c) the trailing edge. For this reason four pressure taps located respectively at 0%, 2.4%, 30% and 90% have been chosen for the upper side of the wing and four pressure taps located respectively at 1.2%, 2.4%, 30% and 90% have been chosen for the lower side of the wing.

A filter has been applied to the computed pressure time histories in order to remove the high-frequency numerical “noise” which has turned out to affect the raw results. For this purpose, only the first 10 harmonics of the Fourier series expansion have been kept. In consideration of the fact that the main frequency is equal to 22.7 Hz, this procedure has implied the removal of the frequencies greater than 227 Hz, a value which has been judged as acceptable in comparison with the mild unsteadiness of the flow filed for this test case.

Both the numerical and experimental pressure time histories at wing sections 1 and 2 have indicated a substantial steadiness of the flow field in this region and for this reason these results have not been reported. Indeed, the numerical investigation has indicated a propeller wake influence from section 3 to the wing tip with a radial wake boundary contraction at the wing trailing edge equal to 87% (Fig.6).

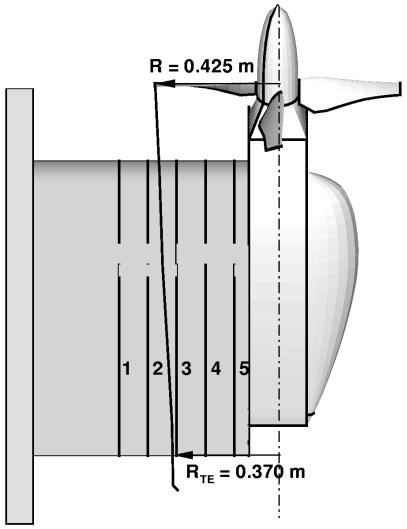

Figure 6: Radial wake boundary contraction

The global analysis of the experimental pressure time signals (Figs.9 and 10) indicate that the unsteadiness of the flow on the wing is basically concentrated at the leading edge (taps 1, 2, 20, 19) with higher amplitudes on the lower side of the wing. A substantial steadiness of the flow can be observed in the central region and at the trailing edge of the upper side of the wing (taps 7 and 10) whereas a small amplitude unsteadiness can be observed at taps 11 and 14 on the lower side of the wing. A 4/rev periodicity, resulting from the propeller blade passages in front of the wing, is in general detected at sections 3 and 5 whereas section 4 exhibits a signal where this periodicity is lost.

The global analysis of the numerical results indicate a general qualitative agreement with the experiment. Differences consisting in some phase shifts (tap 1 – section 3; tap 2 – section 5) and different amplitudes (tap 1 – sections 3 and 5; tap 19) are likely to be due to the different prediction of the blade tip vortex strength and location of the impingement region with the wing. Unlike the experimental results a 4/rev is always detectable in the numerical results.

Conclusions

The aim of this paper was to illustrate the results obtained by CIRA during the pre-test activity of the TILTAERO project and for which the experimental database produced during the PROPWING project was employed for the comparisons.

The following conclusions have been drawn from the present study:

1. The PROPWING database has shown its full effectiveness to highlight the main interactional problems affecting a tilt rotor-like configuration;

2. The presence of a nacelle of big dimensions and set at a high tilt angle, has shown to greatly influence the flow field acting on the wing and to require, at least from panel methodologies, a proper wake modelling to prevent from erroneous predictions of the pressures distributions on the wing surface;

3. The wake modelling applied in RAMSYS has demonstrated its effectiveness even though some further investigation is still needed;

4. The analysis of the time-averaged quantities has confirmed the good prediction capabilities of the methodology applied as far as the global aspects of the interactional phenomenology are concerned;

5. The comparison in terms of the unsteady pressure signals has indicated the ability of the methodology to correctly detect the wing regions affected by higher unsteadiness;

6. The detailed agreement in terms of amplitude and phase has not always been reached and an improvement is mainly required in the interactional process between the blade tip vortices and the wing;

7. The indications obtained by this comparative study have met the main target of the TILTAERO pre-test activity and provide a useful guideline for a correct modelling of the interactional aerodynamics of the TILTAERO wind tunnel model.

Acknowledgments

This work is partly supported by the European Union under the Competitive and Sustainable Growth Programme in the 5th Framework, Contract Nr. G4RD-CT-2001-0047 (TILTAERO project). Furthermore, the author wishes to thank Mr. A. Saporiti of Agusta S.p.A. for providing some results of their numerical investigation of the PROPWING configuration.

References

[1.] Agusta S.p.A., “Tilt Rotor Interactional Aerodynamics – TILTAERO – Project Nr. GRD1-2000-25610 : Annex I, Description of Work,” December 2000;

[2.] Voutsinas, S.G., “PROPWING Final Report,” Feb. 1993;

[3.] Voutsinas, S.G., “The PROPWING Database,” Doc. Nr. TILTAERO/WP1/NTUA/R-01/B, January 2002;

[4.] Fratello, G., Favier, D., Maresca, C., "Experimental and numerical study of the propeller/fixed wing interaction," Journal of Aircraft, Vol. 28, n° 6, pp. 365-373, 1991;

[5.] Chiaramonte, J.Y., Favier D., Maresca C., Benneceur S., "Aerodynamics interaction of the propeller/wing ensemble for different flight configurations," Journal of Aircraft., Vol. 33, n° 1, pp. 46-53, 1996;

[6.] Visingardi, A., D'Alascio, A., Pagano, A., Renzoni, P., "Validation of CIRA's Rotorcraft Aerodynamic Modelling SYStem with DNW Experimental Data," 22nd European Rotorcraft Forum, Brighton, UK., Sep. 1996;

[7.] D'Alascio, A. Visingardi, and P. Renzoni, "Explicit Kutta Condition Correction for Rotary Wing Flows," 19th World Conference on the Boundary Element Method, Rome, Italy, Sep. 1997;

[8.] D.R. Clark, and B. Maskew, "Calculation of Unsteady Rotor Blade Loads and Blade/Fuselage Interference," II International Conference on Rotorcraft Basic Research, College Park, U.S.A., Feb. 1988;

[9.] Nathman, J.K., "VSAERO, A Computer Program for Calculating The Non Linear Aerodynamic Characteristics Of Arbitrary Configurations", User's Manual, Version 6.2, June 2001.

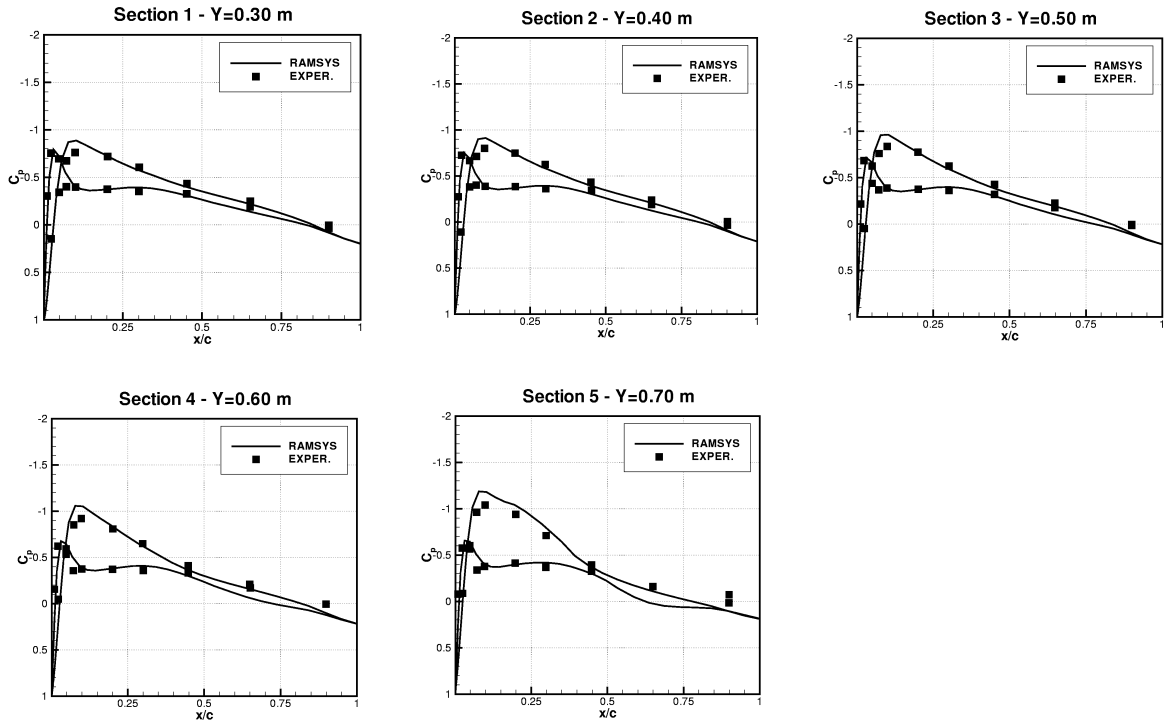

Figure 7: Steady pressure distributions on the wing

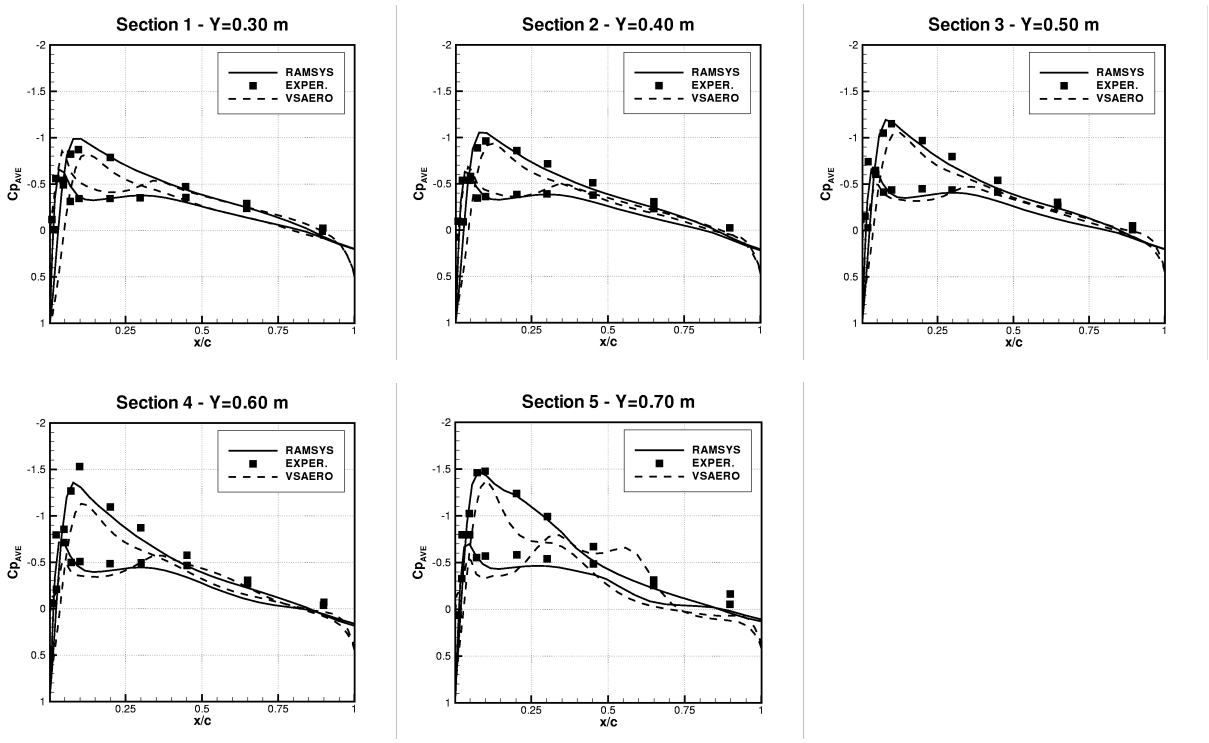

Figure 8: Time-averaged pressure distributions on the wing

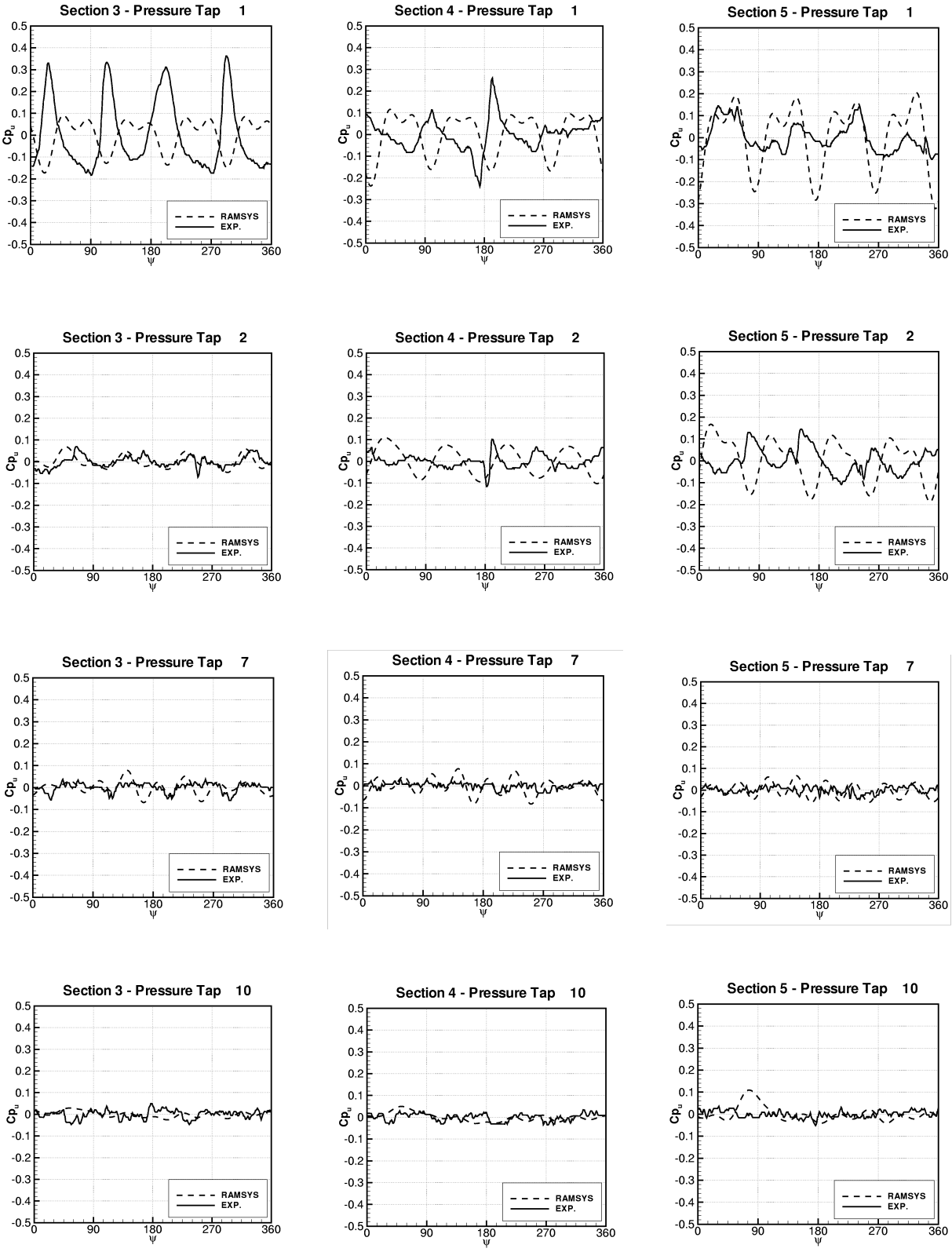

a) Section 3 b) Section 4 c) Section 5

Figure 9: Unsteady pressure coefficient time history on the Upper side of the wing

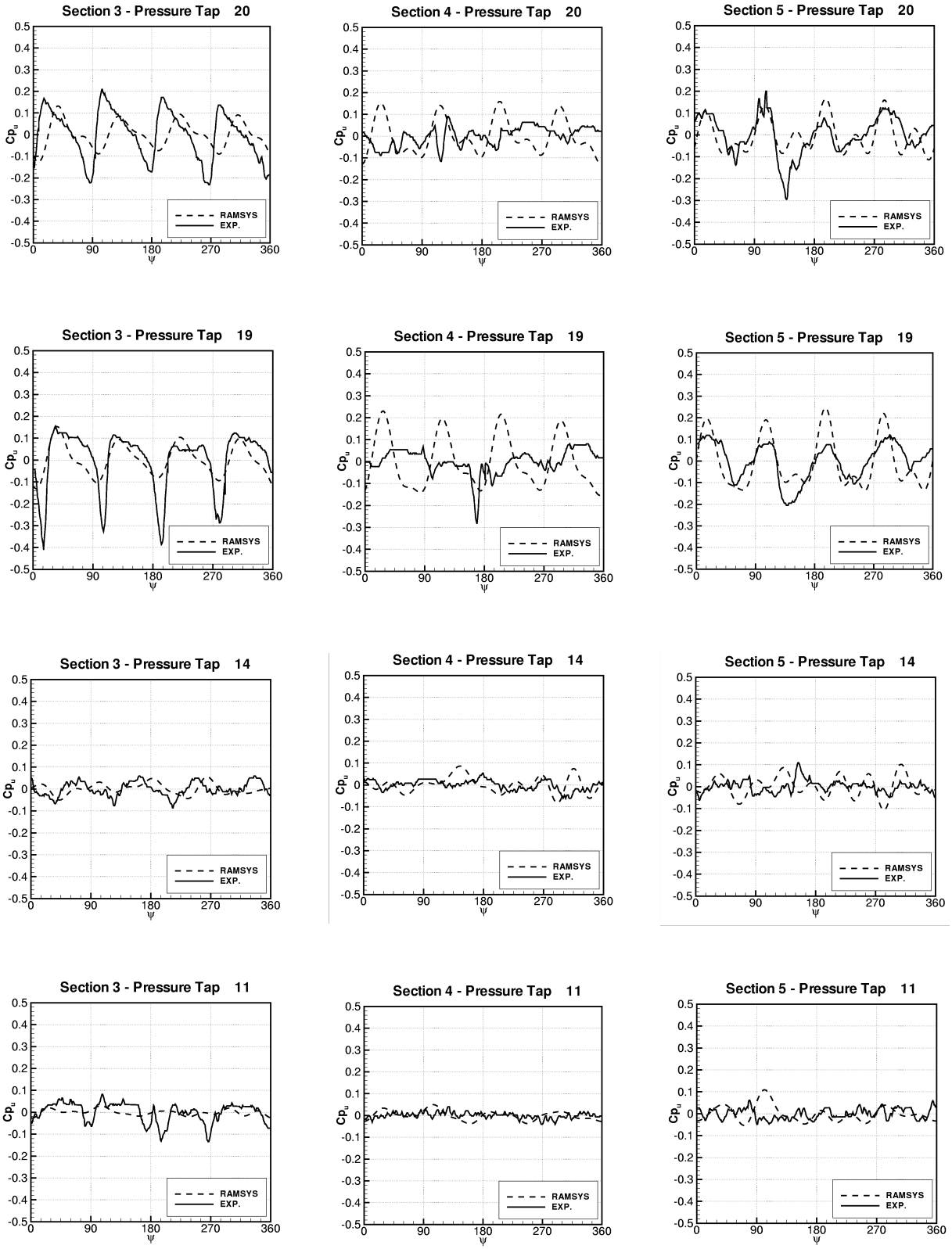

a) Section 3 b) Section 4 c) Section 5

Figure 10: Unsteady pressure coefficient time history on the Lower side of the wing